Frontiers of Environmental Science & Engineering
2025, 19(4): 52 https://doi.org/10.1007/s11783-025-1972-0

RESEARCH ARTICLE

Enhanced resistance to ciprofloxacin stress in integrated floating film activated sludge system filled with surface-modified carriers for simultaneous nitrification and denitrification

Jing Liu, Zepeng Wang, Tao Liu ✉, Xie Quan

Key Laboratory of Industrial Ecology and Environmental Engineering (Ministry of Education), School of Environmental Science and Technology, Dalian University of Technology, Dalian 116024, China

HIGHLIGHTS

- Modified carriers promoted SND resistance to CIP stress with IC_{50} of 36.54 mg/L.
- Modified carriers induced more EPS to trap CIP to mitigate the toxicity.
- Activities of AMO, NXR, NAR, and NIR were less suppressed on modified carriers.
- Target preventing and efflux pumping were the main mechanisms to resist CIP.

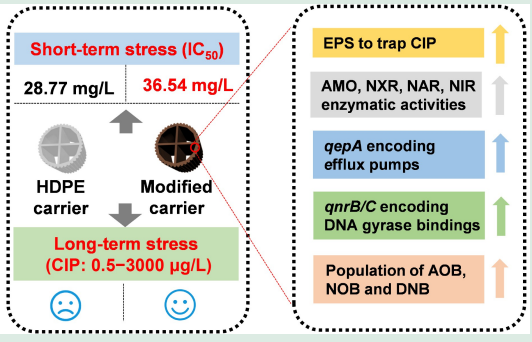

ABSTRACT: While the effectiveness of integrated floating film activated sludge (IFFAS) system filled with surface-modified carriers has been demonstrated in promoting simultaneous nitrification and denitrification (SND) performance, the effect of antibiotic stress on this system remains unexplored. Herein, this study investigated the stress response of SND in IFFAS under short- and long-term exposure to ciprofloxacin (CIP), a commonly used antibiotic. Results indicated the significantly higher semi-inhibitory concentration of CIP in the IFFAS system with modified carriers (36.54 mg/L) than that in IFFAS with conventional high density polyethylene (HDPE) carriers (28.77 mg/L). IFFAS system with modified carriers exhibited improved resistance to CIP toxicity compared to IFFAS using HDPE carriers or conventional activated sludge under long-term exposure to CIP concentrations from 50 to 3000 μg/L. The surface-modified carriers demonstrated a multifaceted strategy to mitigate the inhibitory effects of CIP, such as enhancing production of extracellular polymeric substances (EPS) to serve as a potential protective barrier against CIP toxicity, the less suppression of key enzyme activities involved in nitrogen removal, as well as inducing the upregulation of antibiotic resistance genes (ARGs) (*qepA*, *qnrB/C*) and the integrase gene (*intI1*) to enhance target prevention and efflux pumping mechanisms for resistance to CIP. These findings collectively underscored the efficacy of modified carriers in attenuating CIP toxicity within the SND system.

KEYWORDS: Simultaneous nitrification and denitrification (SND), Ciprofloxacin, Modified carrier, Resistance, Extracellular polymeric substances (EPS)

✉ Corresponding author. E-mail: taoliu@dlut.edu.cn (T. Liu)

Article history: Received 15 December 2024, Revised 17 January 2025, Accepted 18 January 2025, Available online 20 February 2025

1 Introduction

Simultaneous nitrification and denitrification (SND) is a promising nitrogen removal process that integrates aerobic nitrification and anoxic denitrification within a single reactor. SND reduces energy consumption and footprint, making it as an energy-efficient nitrogen removal process for wastewater treatment plants (WWTPs). However, recent investigations have documented the widespread presence of various antibiotics in wastewater, stemming from the escalating discharge of pharmaceuticals into the environment. Despite WWTPs serve as core facilities for antibiotic reception and transmission, they are not specifically designed to effectively treat and remove these antibiotics (Su et al., 2024). It has been reported that a significant portion of antibiotics are absorbed by sludge, while biodegradation plays a relatively minor role during SND process (Jia et al., 2012). The bacteriostatic properties of residual antibiotics in sludge inevitably impact bacterial metabolic pathways, posing a critical challenge to the sustainable operation and maintenance of SND (Michael et al., 2013).

Among the antibiotics, ciprofloxacin (CIP) is a kind of broad-spectrum fluoroquinolones (FQs) that demonstrates antibacterial efficacy against a wide range of both Gram-positive and Gram-negative bacteria (Porras et al., 2016). Its antibacterial mechanism involves inhibiting bacterial DNA gyrase and topoisomerase IV, thereby disrupting DNA replication and leading to cell death (Martínez, 2008). In China, CIP holds the position of the second most widely used FQs, widely utilized for preventing and treating bacterial infections in humans, livestock, and aquaculture (Zhang et al., 2015; Zhao et al., 2024). While a portion of CIP is metabolized within the body, a substantial proportion (up to 72%) is excreted in its pharmacologically active form (Zhang et al., 2015). The ubiquitous presence of CIP has been reported in various wastewater sources. It has been documented that the concentrations of CIP ranged from 15 ng/L to 246 μg/L in domestic wastewater, 2–24 μg/L in hospital wastewater, and 28–31 mg/L in pharmaceutical industry wastewater (Nguyen et al., 2017; Tran et al., 2018).

Previous research has investigated the toxic effects of CIP on SND, including decreasing species diversity, altering the phylogenetic structure, decreasing the abundance of dominant denitrifying bacterial genera and low- or non-expressing genes associated with nitrification and denitrification (Kim et al., 2020; Li et al., 2021). However, these studies primarily focused on sludge-based SND systems. The potential impact of CIP on SND within biofilm systems remains largely unexplored. Biofilm offers a distinct micro-environment compared to activated sludge, characterized by a defined thickness and a dissolved oxygen gradient that favor the coexistence of aerobic nitrifiers and anoxic denitrifiers (Flemming et al., 2016). Furthermore, biofilms exhibit unique emergent properties, including synergistic interactions among bacteria, enhanced horizontal gene transfer, and facilitated extracellular polymeric substance (EPS) production (Chen et al., 2024). Biofilms also possess more robust and dense microbial structures, resulting in higher biomass concentration and greater resilience to shock loads. These factors suggest that biofilms may exhibit increased resistance to CIP compared to activated sludge. Therefore, a comprehensive investigation of CIP toxicity on SND within biofilm systems is crucial to understand the potential implications of antibiotic contamination.

In biofilm-based SND systems, carriers play important roles in promoting biofilm formation and nitrogen removal performance. Research has demonstrated that different bacteria exhibit distinct preferences for carrier surfaces with specific properties (Khan et al., 2013). Leveraging this principle, the development of surface-modified carriers with tailored properties presents a promising strategy for the *in situ* selective enrichment of autotrophic nitrifiers, which is crucial for maintaining big populations of these slow-growing microorganisms within the system. Previous research has demonstrated the substantial ammonium adsorption capacity of zeolite (Li et al., 2020). Additionally, zeolite's hydrophilic feature can promote the formation of nitrifying biofilms (Nguyen et al., 2016). On this basis, certain amount of zeolite was added into conventional carriers to prepare surface-modified carriers in our previous study (Jing et al., 2019). The surface-modified carriers based integrated floating-film activated sludge (IFFAS) system exhibited superior enrichment of nitrifying bacteria and enhanced SND performance compared to the conventional high density polyethylene (HDPE) carriers based IFFAS system (Liu et al., 2018). However, the resistance of modified carriers to CIP stress compared to conventional carriers remains unknown. This study posits that the augmented biomass and complex structure of modified carriers could contribute to enhanced tolerance against CIP stress, suggesting their potential use in SND for treating wastewater containing antibiotics.

Herein, this study investigated the stress response of SND in IFFAS filled with modified carriers under short- and long-term exposure to CIP. The investigation

focused on the characterization of EPS, community structure shifts, activities of key enzymes involved in nitrogen removal, abundance of nitrogen-removal related genes and antibiotic resistance genes (ARGs) in response to varying CIP concentrations. The findings were anticipated to provide insights into the stress response mechanisms of IFFAS process filled with modified carriers under CIP exposure, and highlight the potential application for treating wastewater containing antibiotics.

2 Materials and methods

2.1 IFFAS configuration and long-term operational condition

Three laboratory-scale reactors were set up, including R0 (filled with activated sludge), R1 (filled with HDPE carriers) and R2 (filled with modified carriers). The height was 32 cm, diameter was 15 cm and working volume was 5.3 L. The filling rate of carriers was 30%. Preparation process of HDPE carriers and modified carriers could be referred to Jing et al. (2019).

Three reactors were operated in a sequential batch mode with the hydraulic retention time (HRT) of 8 h. Each cycle consisted inletting (10 min), aeration (100 min), hypoxia (380 min) and discharging (10 min). In aerobic phase, an aeration pump (ACO-004, Sunsun, Hangzhou, China) was used to continuously introduce oxygen and maintain the dissolved oxygen (DO) concentration of 2.0–4.0 mg/L. Stirrers (LC-ES-200SH, Licheng, Shanghai, China) were used in R1 and R2 to ensure carrier fluidization. The temperature was controlled to be 28–30 °C using a water bath. Seeding sludge was obtained from the secondary sedimentation tank of a WWTP in Dalian, China. Sludge was regularly discharged on a weekly basis to maintain a mixed liquor suspended solids (MLSS) concentration of approximate 3500 mg/L.

The synthetic wastewater was formulated to contain 300 mg/L COD in the form of glucose, 60 mg/L ammonia nitrogen (NH_4^+-N), 6 mg/L KH_2PO_4, 15 mg/L $CaCl_2{\cdot}2H_2O$, 15 mg/L $MgSO_4{\cdot}7H_2O$, and 1 mL/L Wolfe's trace element solution. The reagents (AR) used in the synthetic wastewater were purchased from Damao Chemical Reagent Partnership Enterprise, Tianjin, China. pH was controlled at 7.5 ± 0.4. The experimental process lasted 120 d, which were divided into five phases according to different CIP concentrations. Phase I served as a control with no CIP introduced. After 20 d of operation, the effluent nitrogen compound concentrations of all three reactors exhibited stable trends, suggesting that the microbial structure within the reactors had attained a relatively stable condition. Afterwards, the concentrations of CIP were 0.5 μg/L in phase II (day 21–45), 50 μg/L in phase III (day 46–70), 300 μg/L in phase IV (day 71–95) and 3000 μg/L in phase V (day 96–120). The selected CIP concentration (0.5–3000 μg/L) was based on those reported levels in real wastewaters (Lindberg et al., 2004; Guo et al., 2017). CIP (AR) was purchased from J&K Scientific Co., Ltd., Beijing, China.

2.2 Short-term configuration and operational condition

The random sample containing 20 g sludge and 100 pieces of carriers were collected from R1 and R2, respectively. These samples were then distributed evenly into serum bottles, with each bottle containing 0, 5, 10, 25, and 50 mg/L of CIP, respectively. The bottles were filled with the same synthetic wastewater used in the long term experiment. Water samples were extracted every 2 h using a sterile syringe. Concentrations of COD, NH_4^+-N, NO_3^--N, NO_2^--N, and total nitrogen (TN) were measured. The composition and fluorescence properties of EPS were also analyzed. The TN removal rate (TNRR, mg N/(gVSS·h)), specific ammonia oxidation rate (SAOR, mg N/(gVSS·h)) and inhibition proportion (IP, %) were calculated using Eqs. (1)–(3), respectively. The semi-inhibitory concentration (IC_{50}) represented the concentration of CIP at which IP was 50%, which was derived from the model fitting of the IP data.

$$TNRR = (C_{\text{TN initial}} - C_{\text{TN end}})/(t \times VSS), \quad (1)$$

$$SAOR = (C_{\text{NH}_4\text{ initial}} - C_{\text{NH}_4\text{ end}})/(t \times VSS), \quad (2)$$

$$IP = (TNRR_0 - TNRR_i)/TNRR_0 \times 100\%, \quad (3)$$

where $C_{\text{TN initial}}$ and $C_{\text{TN end}}$ were the TN concentrations at the beginning and end of the period (mg N/L); $C_{\text{NH}_4\text{ initial}}$ and $C_{\text{NH}_4\text{ end}}$ were the NH_4^+-N concentrations at the beginning and end of the period (mg N/L); t was time (h); VSS was volatile suspended solid (g/L); $TNRR_0$ was the TN removal rate in the absence of CIP stress; $TNRR_i$ was the TN removal rate under the influence of CIP stress.

2.3 Analytical methods

The concentrations of NH_4^+-N, NO_3^--N, NO_2^--N, TN, COD, MLSS, and MLVSS were analyzed using the methods specified in Discharge standard of pollutants for municipal wastewater treatment plant (GB18918-2002). DO was measured by a portable instrument

(model 55/12, YSI, USA) and pH was detected by a pH meter (PB-10, Sartorius, Germany). EPS was extracted from the sample, and polysaccharide (PS) contents were determined using the phenol-sulfuric acid while protein (PN) contents were quantified by modified Lowry method (Liu et al., 2021). Fluorescence properties of the EPS were characterized by three-dimensional excitation-emission matrix spectra (3D-EEM) using a fluorescence spectrometer (Cary Eclipse, Agilent, USA). Parallel factor analysis (PARAFAC) was employed to analyze the 3D-EEM data (Li et al., 2008).

2.4 Key enzyme activity assay

The enzymatic activities of key enzymes for nitrification and denitrification were quantified. These enzymes included ammonia monooxygenase (AMO), nitrite oxidoreductase (NXR), nitrate reductase (NAR) and nitrite reductase (NIR). An enzyme-linked immunosorbent assay (ELISA) was used for this quantification. The ELISA kits were purchased from LMAI Bio Co. Ltd., Shanghai, China.

2.5 Bacterial community structure and functional genes analysis

Samples of sludge and biofilm were collected at phase I and phase V. The microbial community structures were investigated using high throughput sequencing. The general primer pair 341F/805R was used to amplify the V3–V4 hypervariable region of the 16S rRNA gene. Subsequently, Illumina Miseq platform (Sangon, China) was employed for sequencing the PCR products. Stringent quality control measure was implemented to filter raw data and obtain high-quality sequences. Bacterial community composition was determined by clustering the effective sequences based on taxonomic classification. Phylogenetic Investigation of Communities by Reconstruction of Unobserved States (PICRUSt2) was utilized to predict bacterial functional pathways. Functional gene annotation was carried out using the Kyoto Encyclopedia of Genes and Genomes (KEGG) databases (Biswal et al., 2020). The Functional Annotation of Prokaryotic Taxa (FAPROTAX) tool was used to predict functional metabolic pathways.

2.6 Resistance genes quantification

ARGs (*qepA*, *qnrA*, *qnrB* and *qnrC*) and one integrase gene (*intI1*) were quantified using quantitative polymerase chain reaction (qPCR) (480II, Roche, USA). The applied primer sequences were provided in Table S1.

3 Results and discussion

3.1 Short-term effect of CIP on SND performance and EPS contents

Short-term effect of CIP on SND performance and EPS contents in HDPE carrier group and modified carrier group was shown in Fig. 1. Initially, without the addition of CIP, SAORs in HDPE carrier group and modified carrier group were comparable. However, as CIP concentrations increased to 5, 10, 25, and 50 mg/L, a consistent decline in SAORs was observed in both HDPE carrier group and modified carrier group (Fig. 1(a)). This decline suggested that CIP inhibited the activity of nitrifying bacteria in the system. Notably, at CIP concentrations of 5 and 10 mg/L, the SAORs in both reactors remained statistically similar. However, at higher CIP concentrations (25 and 50 mg/L), the SAORs in modified carrier group were 1.62 and >1.26 mg N/(gVSS·h), while those in HDPE carrier group were 1.69 and 1.41 N/(gVSS·h), respectively. This divergence indicated that nitrifying bacteria in modified carrier group exhibited superior tolerance to higher CIP concentrations compared to those in HDPE carrier group. Figure 1(b) demonstrated a significantly higher TNRR in modified carrier group than in HDPE carrier group, which highlighted the role of modified carriers in promoting TN removal performance. Model fitting results (Fig. 1(c)) indicated that IC_{50} of HDPE carrier group and modified carrier group were 28.77 and 36.54 mg/L, respectively. This result indicated that modified carrier group had a stronger resistance to CIP compared to HDPE carrier group, which was probably attributed to the addition of modified carriers. COD removal efficiency was almost constant when the CIP concentration was increased (Fig. 1(d)), demonstrating the increased CIP concentrations had negligible impact on COD removal performance.

The EPS contents and compositions in sludge and biofilm samples at different CIP levels were shown in Figs. 1(e) and 1(f). EPS content in the sludge remained relatively stable at CIP concentrations below 25 mg/L. However, a significant increase in EPS content within the sludge was observed at the CIP concentration of 50 mg/L. Moreover, the EPS content in the sludge within modified carrier group consistently surpassed that in HDPE carrier group. For the biofilm on carriers, an increased concentration of CIP resulted in a corresponding increase in EPS contents within both HDPE carrier group and modified carrier group. The increased production of EPS facilitated the relocation of CIP to specific binding sites within the EPS matrix, thereby shielding the microorganisms from CIP

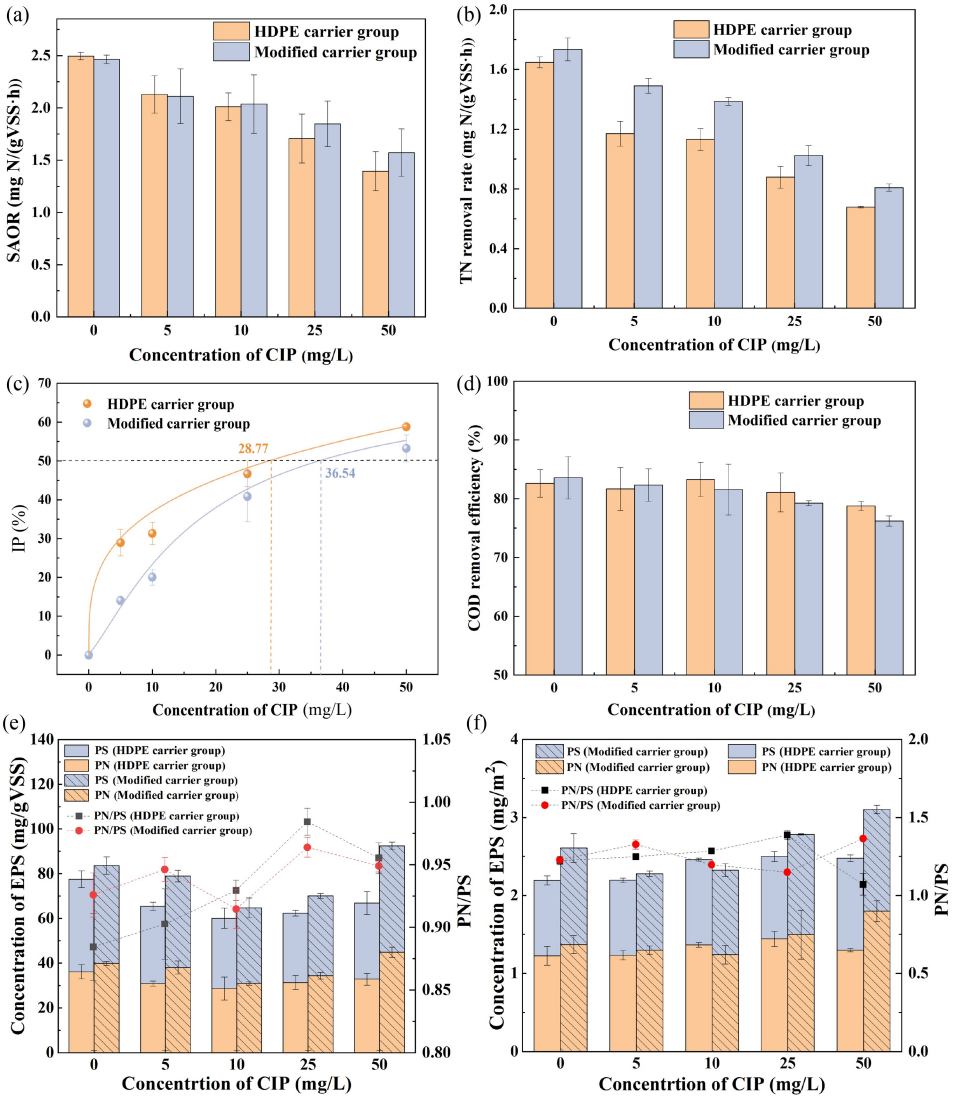

Fig. 1 Short-term effect of CIP on SAOR (a), TNRR (b), IP (c), COD removal efficiency (d), and EPS contents of suspended sludge (e) and biofilm (f).

inhibition (Zhang et al., 2023). Notably, a higher concentration of CIP (25 and 50 mg/L) led to a significant increase in EPS production on the modified carrier, suggesting a potentially enhanced protective effect. This heightened EPS content might be a key factor contributing to the increased IC_{50} value in modified carrier group (36.54 mg/L) compared to HDPE carrier group (28.77 mg/L). The PN/PS ratio of HDPE carrier group sludge exhibited a positive correlation with increasing CIP concentration, suggesting a shift toward a more hydrophobic EPS under CIP stress (Mahendran et al., 2012). However, the PN/PS ratio in modified carrier group sludge, biofilm on HDPE carrier and biofilm on modified carrier remained relatively constant, implying a less pronounced effect of CIP stress on EPS composition in these systems.

Two components (C1 and C2) of EPS were recognized by PARAFAC analysis (Fig. S1). C1 (Ex/Em: 320/388 nm) was identified as humic-like substances. C2 displayed two peaks at Ex/Em of 235/360 nm and 280/360 nm, which were identified as aromatic amino acid tryptophan and tyrosine of protein-like substances, respectively. PARAFAC results indicated the quenching constants (Kq, L/(mol·s)) for both C1 and C2 exceeded 2.0×10^{10} L/(mol·s), surpassing the maximum diffusion collision quenching rate constant for quenchers interacting with biological macromolecules. This result suggested a static quenching mechanism, where the decrease in

fluorescence intensity was attributed to the formation of non-fluorescent complexes between CIP and humic substances (C1) / protein-like substances (C2). Consequently, the quenching phenomenon was not driven by collisional interactions but rather by the direct complexation of CIP with the EPS components.

3.2 Long-term effect of CIP on SND performance

Long-term effect of CIP on SND performance lasted 120 d. The experiment was designed to encompass five distinct phases, each characterized by varying concentrations of CIP (0–3000 μg/L) (Fig. 2). In phase I (without CIP), all reactors (R0, R1, and R2) exhibited stable NH_4^+-N (Figs. 2(a) and 2(b)) and TN (Figs. 2(c) and 2(d)) removal efficiencies. TN removal efficiencies (TNREs) were 73.13%, 78.39%, and 78.36% for R0, R1, and R2, respectively. The corresponding TNRR averaged 3.24 ± 0.26 mg N/(gVSS·h) in R0, 3.44 ± 0.21 mg N/(gVSS·h) in R1 and 3.75 ± 0.28 mg N/(gVSS·h) in R2. Notably, the highest TNRR observed in R2 indicated the potential enhancement in nitrogen removal due to the modified carriers, which was in accordance with previous findings (Liu et al., 2018). In phase II (CIP concentration: 0.5 μg/L), the removal efficiencies of NH_4^+-N and TN exhibited a gradual decline during the initial 10 d, followed by a recovery from day 31 to 40. This observed trend suggested the potential development of resistance to CIP within the microbial communities responsible for nutrient removal. The average ammonia removal efficiencies (AREs) were 84.02%, 92.28%, and 96.19%, and TNREs were 62.17%, 70.49% and 78.29% in R0, R1, and R2, respectively. These results demonstrated that R2 exhibited superior nitrogen removal performance compared to R1 and R0. Worthy mention that in R2, the nitrogen removal performance in phase II did not exhibit a significant decline compared to phase I. This observation suggested that low-concentration CIP (0.5 μg/L) had minimal inhibitory effects on SND in IFFAS filled with modified carriers. In phase III (CIP concentration: 50 μg/L), TNRR in R0, R1, R2 decreased by 21.12%, 19.19% and 18.87% respectively compared to phase II. It indicated a notable inhibitory effect of 50 μg/L CIP on the nitrogen removal process. However, the effluent TN concentration in R2 was lower than that in R1 and R0, suggesting R2 with modified carrier had stronger impact resistance to CIP. In phase IV (CIP concentration: 300 μg/L), the effluent NH_4^+-N concentration increased sharply within the first 13 d (day 71–83). To address this, the aerobic duration was extended from 100 min to 120 min from day 84. This operational adjustment resulted in a significant reduction in effluent NH_4^+-N concentration in the three reactors. Furthermore, the effluent TN concentration in R2 and R3 decreased, with R3 exhibiting a superior TN removal performance compared to R2. However, the TN removal performance in R1 did not show any significant improvement. Fig. S2 illustrated the accumulation of NO_2^--N in R1, implying potential inhibition of nitrite oxidizing bacteria (NOB) or certain denitrifying bacteria under CIP stress of 300 μg/L. In phase V (CIP concentration: 3000 μg/L), the average AREs in R0, R1, and R2 were 45.40%, 63.13%, and 72.19%, respectively. These values represented a significant decrease of 38.76%, 19.47%, and 7.88% compared to phase I. The average TNREs in R0, R1, and R2 were 48.74%, 65.42%, and 73.27%, respectively. The corresponding TNRRs in R0, R1, and R2 were 1.81 ± 0.26, 2.21 ± 0.27 , and 2.50 ± 0.28 mg N/(gVSS·h), exhibiting a decrease of 44.26%, 35.74%, and 33.43% compared to phase I. Figure 2(e) showed the overall TNRR trends of the three reactors. While all reactors exhibited a decrease in nitrogen removal with increased CIP concentration, R2 consistently demonstrated the highest TNRR. This result suggested that the IFFAS filled with modified carriers exhibited enhanced resistance to CIP stress.

As illustrated in Fig. 2(f), COD removal efficiencies in R1 and R2 exceeded that of R0. Notably, the COD removal did not exhibit significant decline with increasing concentrations of CIP. This finding aligned with previous research that demonstrated the CIP concentrations of 500 μg/L did not notably inhibit COD removal when utilizing readily degradable carbon sources (Cai et al., 2022).

3.3 Long-term effect of CIP on EPS contents and composition

The impact of CIP on EPS contents and biofilms properties was investigated. Compared to phase I without CIP addition, EPS production exhibited a gradual increase with increasing CIP concentrations. While there were no significant differences in EPS contents among the sludge samples in three reactors, the EPS contents on the carriers showed a marked increase with increasing CIP concentrations (Fig. 3(a)). Notably, the EPS content on modified carriers consistently exceeded that on conventional carriers. Biofilm biomass also exhibited the similar trend (Fig. 3(b)). The modified carriers with thicker biofilms than conventional carriers (Fig. 3(c)) implied a stronger resistance to CIP stress (Tang et al., 2022). CIP was a type of highly hydrophobic antibiotic, which exhibited a strong affinity for biomass, readily adsorbing through

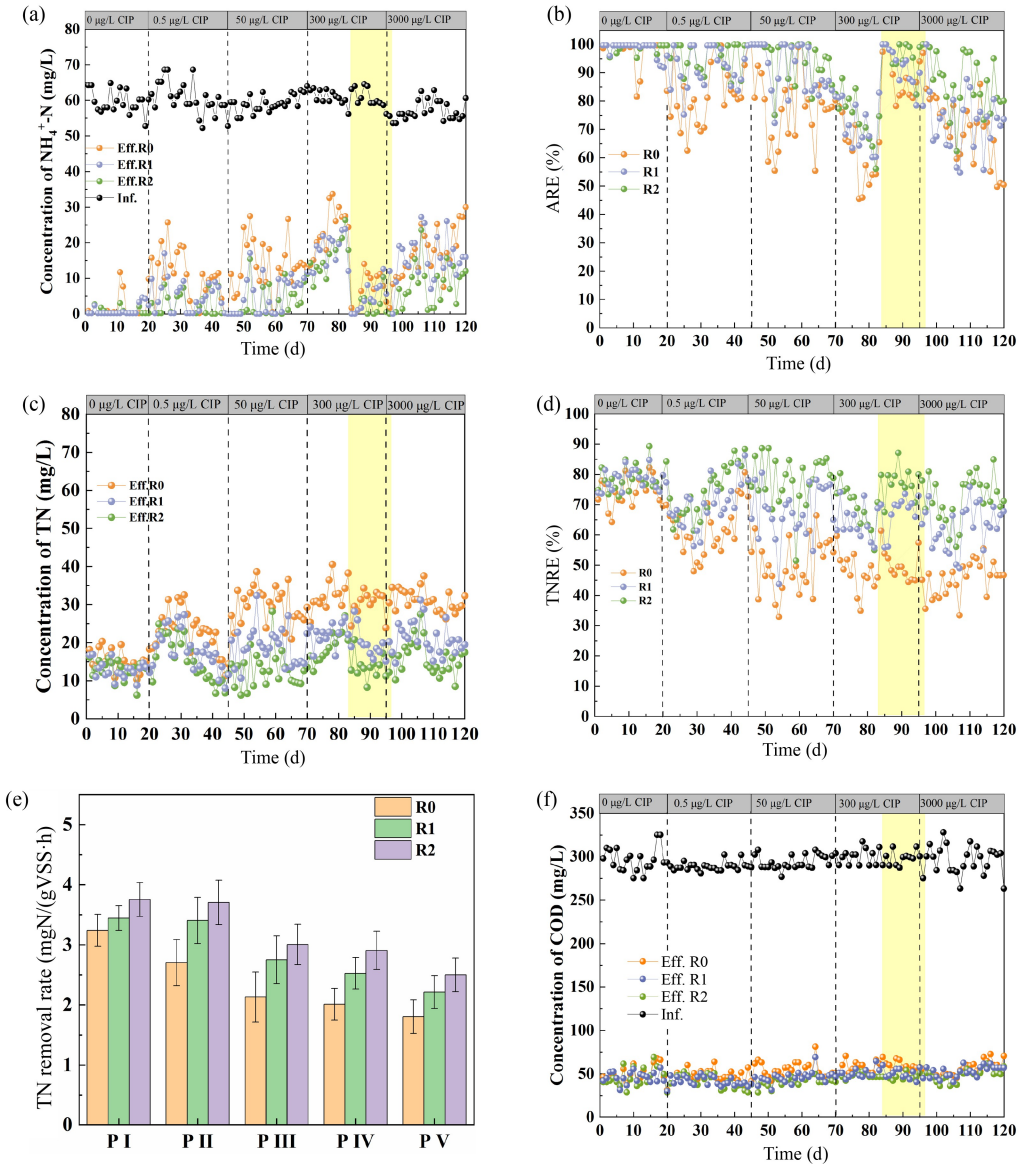

Fig. 2 Nitrogen and COD removal performances during the long-term exposure of CIP: influent and effluent concentration of NH_4^+-N (a), NH_4^+-N removal efficiencies (AREs) (b), influent and effluent concentration of TN (c), TN removal efficiencies (TNREs) (d), TN removal rate (e) and influent and effluent concentration of COD (f). The time period highlighted by the yellow background represented the aerobic duration was adjusted from 100 to 120 min.

both hydrophobic and electrostatic interactions (Amorim et al., 2014). As illustrated in Fig. 3(d), the PN/PS ratios in both sludge and biofilm displayed an increasing trend, indicating enhanced hydrophobicity of the EPS. This heightened hydrophobicity likely facilitated the adsorption of CIP on EPS, thereby mitigating its toxicity to functional microorganisms. Noting that the decreasing trend in PN/PS ratio was observed in phase III compared to phase II. It suggested that PN was more significantly inhibited than PS when exposed to 50 ng/L CIP. This difference might be attributed to CIP inhibitory effect on bacterial DNA gyrase, thereby hindering PN synthesis. However, the increase in PN/PS ratio in phase IV indicated the system's adaptation to mitigate the toxic effects of CIP.

3D-EEM fluorescence spectra of EPS indicated the quenching constant (*Kq*, L/(mol·s)) for C1 exceeded 2.0×10^{10} L/(mol·s) (Fig. S3). The increase in CIP concentrations led to a corresponding decrease in fluorescence intensity of C1 component, suggesting a potential complexation between CIP and humic-like substances (Xu et al., 2013). Unlike those of C1, the

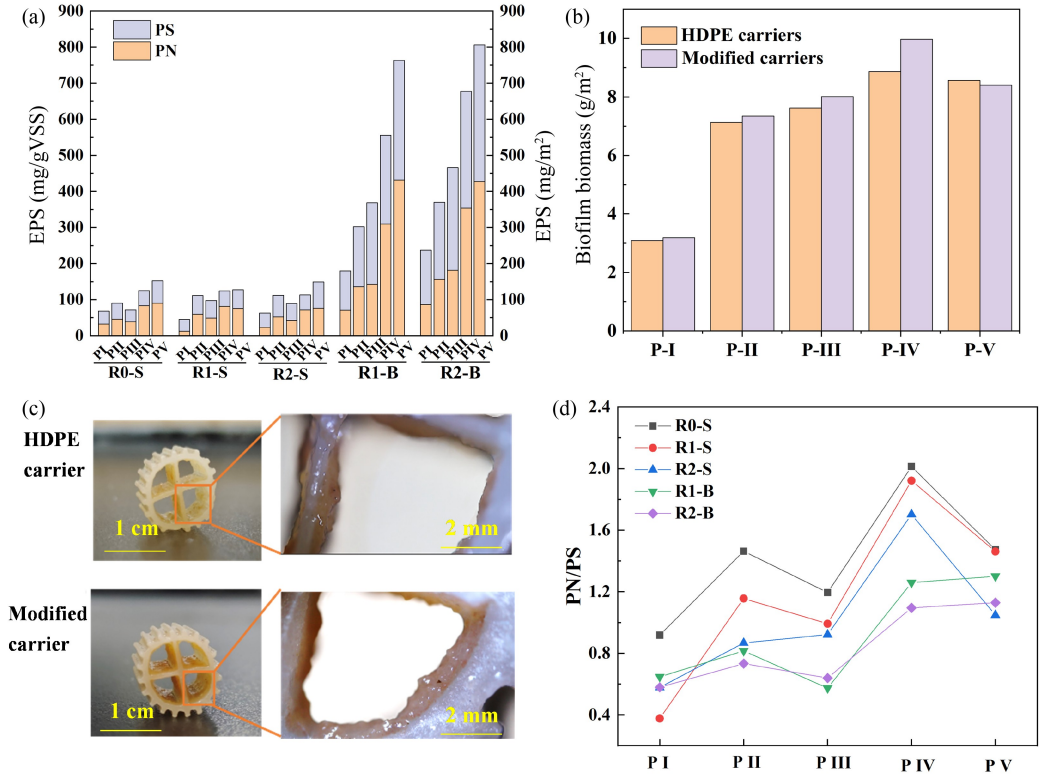

Fig. 3 Variations of EPS content in sludge (mg/g VSS) and on carrier (mg/m^2) (a) and biofilm biomass (b) under long-term stress of CIP. (c): Photos of the carriers in phase IV. (d): PN/PS ratio. R_i-S: sludge sample in R_i; R_i-B: biofilm sample in R_i.

fluorescence intensities of C2 exhibited an increase with increasing CIP additions, indicating that protein-like substances were stimulated in response to the continuous exposure to CIP (Gu et al., 2017).

3.4 Long-term effect of CIP on key enzymes activities

The key enzymes activities involving in nitrification (AMO and NXR) and denitrification (NAR and NIR) in response to CIP were measured. In phase I, a significant amount of sludge transferred to the carrier surface to form biofilms in R1 and R2. Consequently, the activities of four enzymes in the sludge of R1 and R2 decreased compared to R0. However, the decline in the sludge of R2 was significantly less than that in R1, with even the NAR activity slightly increasing compared to R0, highlighting the potential advantage of the modified carrier in maintaining enzyme activity. For biofilm samples in R1 and R2, the nitrifying enzyme activity (AMO, NXR) on the modified carrier was higher than that on HDPE carrier. This could be attributed to the zeolite added in the modified carrier, which effectively adsorbed ammonium from wastewater, thereby promoting nitrification. However, the denitrifying enzyme activity (AMO, NXR) on the modified carrier was not increased compared to that on HDPE carrier. Since the modified carrier was not specifically designed for denitrification, its promoting effect on denitrification was limited. Moreover, Figs. 4(a) and 4(b) demonstrated a marked difference of AMO and NXR activities between sludge and biofilm. In sludge, a significant decrease in AMO and NXR activities was observed in phase II with the addition of 0.5 μg/L CIP. While in biofilm, a decline in AMO and NXR activities was not observed until phase III (CIP concentration: 50 μg/L). This result highlighted the greater resistance of biofilm to CIP than sludge. In phase III, the AMO and NXR activities in biofilm of conventional carriers were reduced by 63.2% and 63.6% respectively compared with phase II. While in biofilm of modified carriers, these reductions were only 4.5% and 17.7%, respectively. It indicated that CIP exerted a more pronounced inhibitory effect on the nitrification activity of conventional carriers compared to modified carriers. This finding was in accordance with the observed NH_4^+-N removal performance depicted in Fig. 2(a). The activities of NAR (Fig. 4(c)) and NIR (Fig. 4(d)) involved in denitrification decreased significantly with the increasing CIP dosing, which was consistent with previous findings (Yi et al., 2017). Nevertheless, the

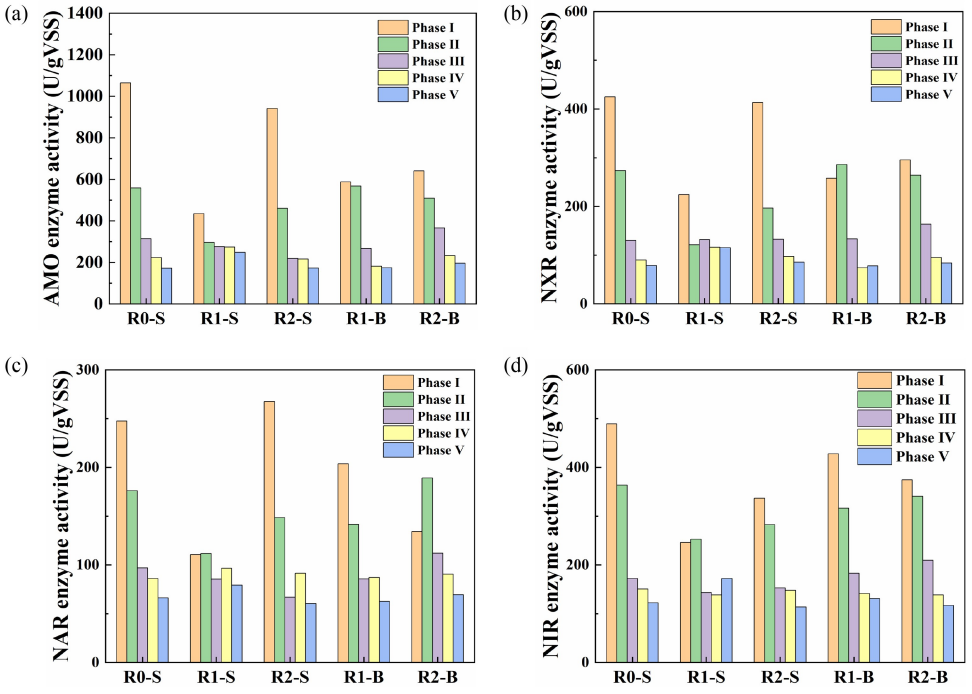

Fig. 4 Enzymatic activities of AMO (a), NXR (b), NAR (c), and NIR (d) in sludge and biofilm in different phases. R_i-S: sludge sample in R_i; R_i-B: biofilm sample in R_i.

activities of NAR and NIR within biofilms on modified carriers were consistently higher than those on HDPE carriers. It indicated the activities of NAR and NIR were less suppressed in the presence of CIP on modified carriers.

3.5 Long-term effect of CIP on microbial community and function genes

High-throughput sequencing analysis was conducted for biofilm and sludge samples collected from phase I (CIP concentration: 0) and phase V (CIP concentration: 3000 μg/L). Chao1 and Ace indexes of all samples except sludge in R2 increased from phase I to V, indicating that the richness in sludge and biofilm increased (Table S2). However, the Shannon index values exhibited a decreasing trend from phase I to V, suggesting a reduction in bacterial community diversity. This decline in diversity was likely a consequence of the increased pressure imposed by CIP.

The microbial community structure at phylum level was presented in Fig. 5(a). In phase I, the dominant phyla were Proteobacteria (19.14%–31.29%), Candidatus Saccharibacteria (13.47%–47.93%), Bacteroidetes (8.98%–12.74%), Acidobacteria (6.03%–11.92%) and Nitrospirae (2.65%–8.41%). In phase V, the relative abundances of Proteobacteria (30.25%–45.99%) and Bacteroidetes (8.09%–30.37%) remained substantial. However, the abundance of Candidatus Saccharibacteria (2.73%–27.66%) significantly decreased, while Firmicutes (1.84%–7.53%) and Unclassified Bacteria (1.32%–10.82%) emerged as notable phyla. These marked alterations in phylum-level demonstrated the profound impact of CIP on microbial community composition.

Nitrosomonas was identified as the functional AOB and *Nitrospira* was identified as the functional NOB in the system (Fig. 5(b)). Moreover, some heterotrophic nitrifiers were also detected, including *Comamonas*, *Chryseolinea* and *Bacillus* (Kim et al., 2005). The relative abundances of these nitrifiers showed a significant decline from phase I to phase V, indicating that CIP had a detrimental effect on the survival of both autotrophic and heterotrophic nitrifiers (Table S3). Different kinds of denitrifying bacteria (DNB) were detected in the system (Table S3). Among them, *Azospira* was identified as the dominant DNB, which showed an increase in relative abundance by 66.39%–86.97% from phase I to phase V, indicating its strong resistance to CIP. This observation aligned with previous research (Zhou et al., 2016). The relative abundance of *Azospira* was typically greater on biofilms than in the sludge, implying biofilm offered a better niche for *Azospira.* However, the relative abundance of other DNB such as *Dokdonella*, *Thauera*, *Zooglea* and *Terrimonas* decreased in phase V

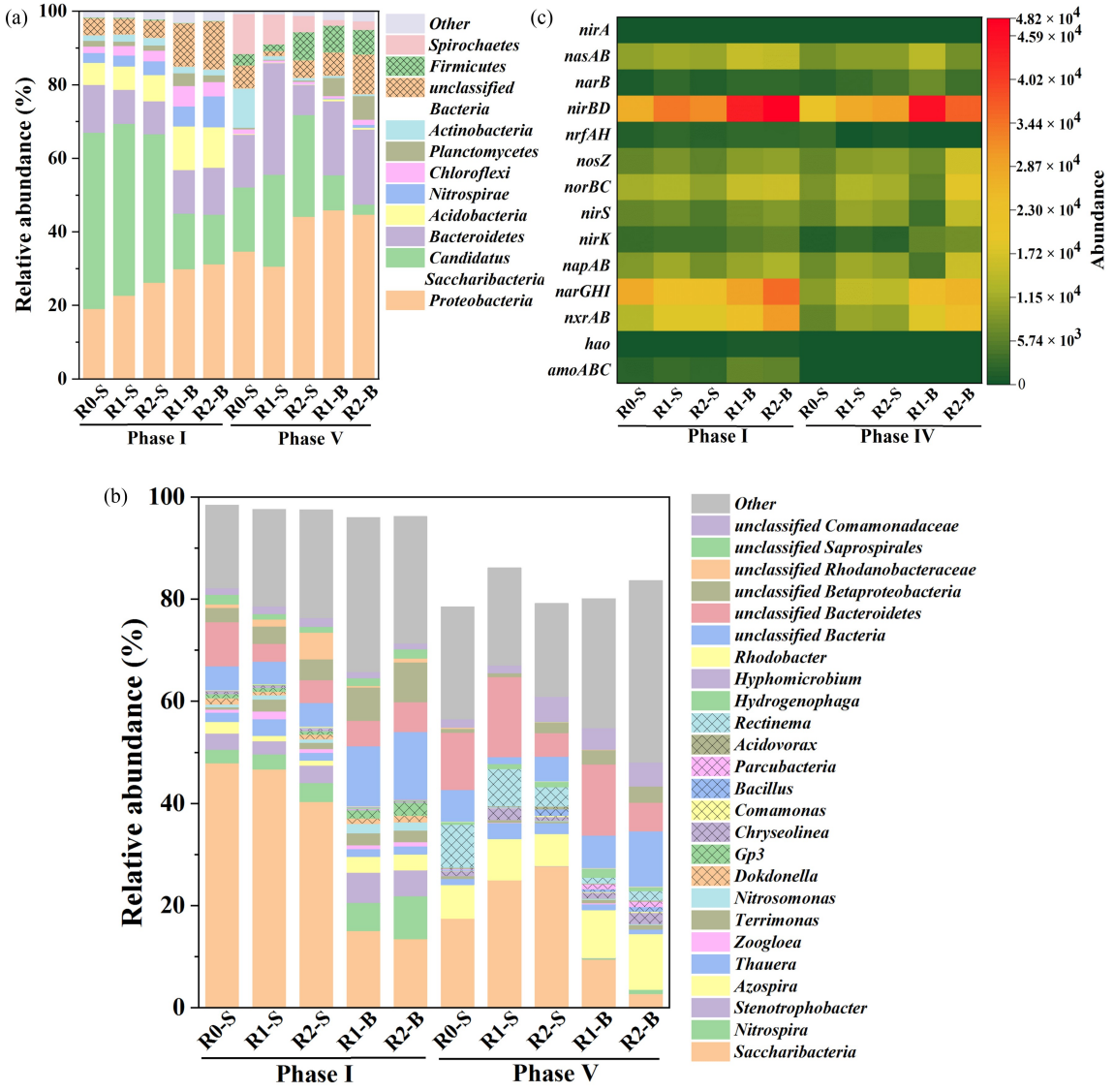

Fig. 5 The relative abundance of bacteria at phylum (a), genus level (b) and heatmap (c) in phase I and V. R_i-S: sludge sample in R_i; R_i-B: biofilm sample in R_i.

compared to phase I, suggesting that long-term CIP stress negatively impacted the survival of these DNB.

Fourteen functional genes associated with nitrogen metabolism (including nitrification, denitrification, nitrate dissimilar reduction to ammonia (DNRA) and nitrate assimilation reduction) were identified (Fig. 5(c)). The genes responsible for ammonia oxidation (*amoABC* and *hao*) and nitrite oxidation (*nxrAB*) displayed a significant decrease in abundance from phases I to V, ranging from 47.88% to 61.07%. Despite this reduction, their abundance on the modified biofilm was 1.27 times higher than that on the HDPE carrier biofilm. This suggested a potential mitigating effect against CIP stress on the modified carriers, potentially contributing to enhanced nitrogen removal capacity. From phase I to V, the abundance of the denitrification genes, including *narGHI*, *napAB*, *nirK*, *nirS*, *norBC*, and *nosZ*, decreased by 16.43%–52.12%. This result indicated a significant reduction in denitrification activity under CIP stress. The genes *nrfAH* and *nirBD* participated in DNRA showed a substantial decrease of 52.55%–60.69%, and the genes *narB*, *nasAB* and *nirA* responsible for nitrate assimilation reduction experienced a reduction in abundance ranging from 6.34% to 60.69%. These results indicated that the genes responsible for nitrification, denitrification, DNRA and nitrate assimilation were downregulated by the addition of

CIP. Nevertheless, it revealed a higher abundance of nitrogen metabolism genes on the modified carriers compared to the HDPE carriers. This observation suggested that the modified carriers possessed the potential to alleviate, to a certain degree, the adverse effects of CIP stress by promoting nitrogen metabolism.

The functional profiling of nitrogen metabolism, as predicted by FAPROTAX, revealed significant shifts in response to CIP exposure (Fig. S4). In the absence of CIP (phase I), the dominant functional groups included aerobic ammonia oxidation, aerobic nitrite oxidation, nitrification, nitrate respiration, nitrate reduction, nitrogen respiration, and chemoheterotrophy. Denitrification exhibited comparatively lower abundance. In phase V, a marked inhibition of aerobic ammonia oxidation, aerobic nitrite oxidation, and nitrification was observed. However, nitrate respiration and nitrate reduction remained largely unaffected. Notably, the abundance of nitrification in R2 biofilm demonstrated a significantly higher level compared to R1 biofilm, indicating that the modified carrier mitigated the inhibitory effect of CIP on nitrification.

3.6 Resistance genes analysis

Four frequently detected ARGs encoding CIP resistance (*qepA*, *qnrA*, *qnrB*, and *qnrC*) and one integrase gene (*intI1*) were quantified in phase I and V (Fig. 6). The gene *qepA* encoded an efflux pump responsible for transporting FQs from the cytoplasm to the bacterial outer membrane (Arakawa, 2020). The copy number of *qepA* gene showed an increasing trend from phase I to V, indicating CIP stimulated the upregulation of *qepA*, thereby facilitating CIP expulsion and reducing bacterial toxicity. It was noted that the *qepA* copy number was consistently higher on the modified carrier compared to the HDPE carrier, suggesting a role of the modified carrier in promoting *qepA* expression. *qnr* genes encode proteins that bind to bacterial DNA gyrase, thereby preventing the antibiotic from interacting with its target (Bush et al., 2020). The modified carrier exhibited a significantly higher copy number of *qnrB* compared to the HDPE carrier, emphasizing its role in promoting microbial resistance. From phase I to V, upregulation of *qnrB/C* indicated that the increase of CIP concentration induced qnr family proteins synthesis. The *intI1* was a common mobile genetic element that possessed the capacity to influence gene expression, thereby potentially contributing to the rapid dissemination of ARGs (Liu et al., 2019). From phase I to V, the copy numbers of *intI1* increased significantly, and R2 exhibited a higher abundance compared to R1 and R0. This suggested that the horizontal transfer of ARGs was enhanced in R2 with increasing concentrations of CIP. It was worth noting that ARGs and the possible accompanist of antibiotic resistant bacteria (ARB) induced by modified carriers might pose inherent environmental hazards. It was consequently crucial to evaluate the potential environmental risks of the ARGs associated with modified carriers.

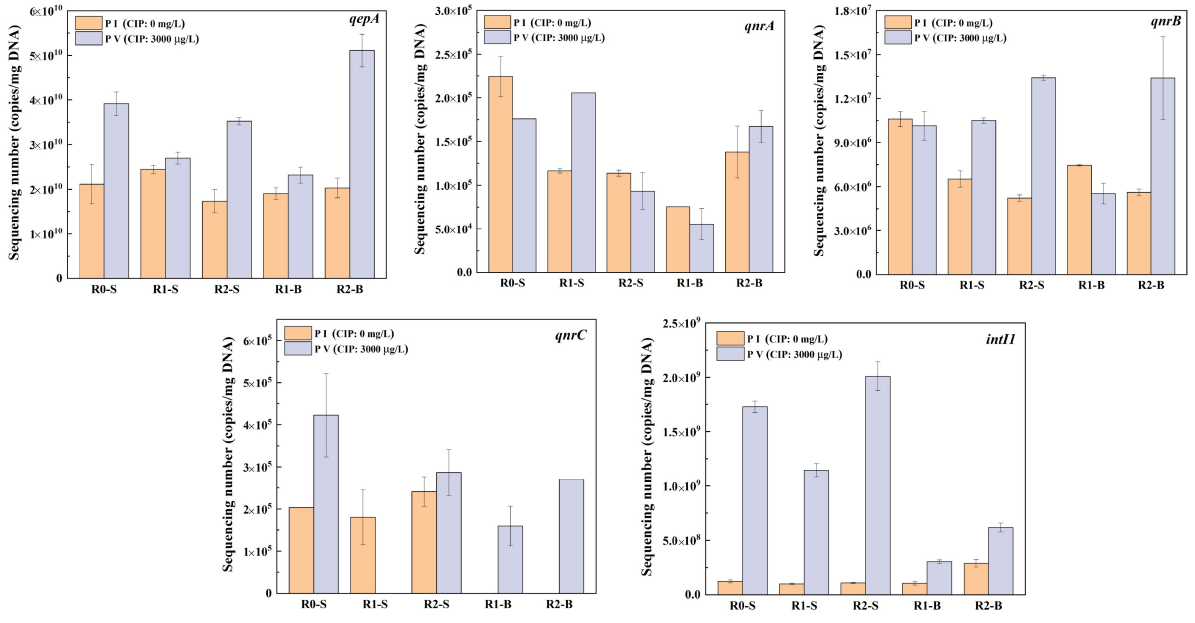

Fig. 6 ARGs and *intI1* copy numbers in phase I and V. R_i-S: sludge sample in R_i; R_i-B: biofilm sample in R_i.

4 Conclusions

IFFAS filled with modified carriers demonstrated a notable enhancement in resistance to CIP toxicity with IC_{50} of 36.54 mg/L, significantly higher than the 28.77 mg/L in the system with HDPE carriers. A low concentration of CIP (0.5 μg/L) did not significantly affect the performance of the SND process. However, prolonged exposure to higher CIP concentrations (50–3000 μg/L) resulted in a substantial inhibition of nitrogen removal activity. The IFFAS system filled with modified carriers demonstrated enhanced resistance to CIP toxicity compared to systems using HDPE carriers or conventional activated sludge. The modified carriers facilitated the formation and aggregation of EPS, effectively trapping CIP and mitigating its toxicity. Moreover, the modified carrier exhibited a higher relative abundance of both nitrifiers and denitrifiers compared to the HDPE carrier. Besides, the activities of key enzymes involved in nitrogen removal were less inhibited in the presence of CIP when using modified carriers. Furthermore, modified carriers induced upregulation of *qepA*, *qnrB/C*, and *intI1*, indicating enhanced target prevention and efflux pumping mechanisms for resistance to CIP. This study provided evidence that the adding of modified carrier into SND system could effectively mitigate CIP toxicity and enhance nitrogen removal performance.

Conflict of Interests The authors declare that they have no known competing financial interests or personal relationships that could have appeared to influence the work reported in this paper.

Acknowledgements This study was supported by the Natural Science Foundation of Liaoning Province of China (No. 2023-MS-099).

Electronic Supplementary Material Supplementary material is available in the online version of this article at https://doi.org/10.1007/s11783-025-1972-0 and is accessible for authorized users.

References

Amorim C L, Maia A S, Mesquita R B, Rangel A O, Van Loosdrecht M C, Tiritan M E, Castro P M (2014). Performance of aerobic granular sludge in a sequencing batch bioreactor exposed to ofloxacin, norfloxacin and ciprofloxacin. Water Research, 50: 101–113

Arakawa Y (2020). Systematic research to overcome newly emerged multidrug-resistant bacteria. Microbiology and Immunology, 64(4): 231–251

Biswal B K, Wang B, Tang C J, Chen G H, Wu D (2020). Elucidating the effect of mixing technologies on dynamics of microbial communities and their correlations with granular sludge properties in a high-rate sulfidogenic anaerobic bioreactor for saline wastewater treatment. Bioresource Technology, 297: 122397

Bush N G, Diez-Santos I, Abbott L R, Maxwell A (2020). Quinolones: mechanism, lethality and their contributions to antibiotic resistance. Molecules, 25(23): 5662

Cai Y, Yan Z, Ou Y, Peng B, Zhang L, Shao J, Lin Y, Zhang J (2022). Effects of different carbon sources on the removal of ciprofloxacin and pollutants by activated sludge: mechanism and biodegradation. Journal of Environmental Sciences, 111: 240–248

Chen Y, Dong K, Zhang Y, Zheng J, Jiang M, Wang D, Zhang X, Huang X, Zhou L, Li H (2024). Enhancing biofilm formation in the hydrogen-based membrane biofilm reactor through bacterial Acyl-homoserine lactones. Frontiers of Environmental Science & Engineering, 18(11): 142

Flemming H C, Wingender J, Szewzyk U, Steinberg P, Rice S A, Kjelleberg S (2016). Biofilms: an emergent form of bacterial life. Nature Reviews. Microbiology, 14(9): 563–575

Gu C, Gao P, Yang F, An D, Munir M, Jia H, Xue G, Ma C (2017). Characterization of extracellular polymeric substances in biofilms under long-term exposure to ciprofloxacin antibiotic using fluorescence excitation-emission matrix and parallel factor analysis. Environmental Science and Pollution Research, 24(15): 13536–13545

Guo X, Yan Z, Zhang Y, Kong X, Kong D, Shan Z, Wang N (2017). Removal mechanisms for extremely high-level fluoroquinolone antibiotics in pharmaceutical wastewater treatment plants. Environmental Science and Pollution Research, 24(9): 8769–8777

Jia A, Wan Y, Xiao Y, Hu J (2012). Occurrence and fate of quinolone and fluoroquinolone antibiotics in a municipal sewage treatment plant. Water Research, 46(2): 387–394

Jing A S, Liu T, Quan X, Chen S, Zhang Y B (2019). Enhanced nitrification in integrated floating fixed-film activated sludge (IFFAS) system using novel clinoptilolite composite carrier. Frontiers of Environmental Science & Engineering, 13(5): 69

Khan M M T, Chapman T, Cochran K, Schuler A J (2013). Attachment surface energy effects on nitrification and estrogen removal rates by biofilms for improved wastewater treatment. Water Research, 47(7): 2190–2198

Kim D, Nguyen L N, Oh S (2020). Ecological impact of the antibiotic ciprofloxacin on microbial community of aerobic activated sludge. Environmental Geochemistry and Health, 42(6): 1531–1541

Kim J K, Park K J, Cho K S, Nam S W, Park T J, Bajpai R (2005). Aerobic nitrification-denitrification by heterotrophic *Bacillus* strains. Bioresource Technology, 96(17): 1897–1906

Li J L, Li J W, Peng Y Z, Wang S Y, Zhang L, Yang S H, Li S (2020). Insight into the impacts of organics on anammox and their potential linking to system performance of sewage partial nitrification-anammox (PN/A): a critical review. Bioresource Technology, 300: 122655

Li W H, Sheng G P, Liu X W, Yu H Q (2008). Characterizing the extracellular and intracellular fluorescent products of activated sludge in a sequencing batch reactor. Water Research, 42(12): 3173–3181

Li Z L, Cheng R, Chen F, Lin X Q, Yao X J, Liang B, Huang C, Sun K, Wang A J (2021). Selective stress of antibiotics on microbial denitrification: Inhibitory effects, dynamics of microbial community structure and function. Journal of Hazardous Materials, 405: 124366

Lindberg R, Jarnheimer P A, Olsen B, Johansson M, Tysklind M (2004). Determination of antibiotic substances in hospital sewage water using solid phase extraction and liquid chromatography/ mass spectrometry and group analogue internal standards. Chemosphere, 57(10): 1479–1488

Liu K, Sun M, Ye M, Chao H, Zhao Y, Xia B, Jiao W, Feng Y, Zheng X, Liu M, et al. (2019). Coexistence and association between heavy metals, tetracycline and corresponding resistance genes in vermicomposts originating from different substrates. Environmental Pollution, 244: 28–37

Liu T, Jia G, Quan X (2018). Accelerated start-up and microbial community structures of simultaneous nitrification and denitrification using novel suspended carriers. Journal of Chemical Technology and Biotechnology, 93(2): 577–584

Liu T, Xu J, Tian R, Quan X (2021). Enhanced simultaneous nitrification and denitrification via adding N-acyl-homoserine lactones (AHLs) in integrated floating fixed-film activated sludge process. Biochemical Engineering Journal, 166: 107884

Mahendran B, Lishman L, Liss S N (2012). Structural, physicochemical and microbial properties of flocs and biofilms in integrated fixed-film activated sludge (IFFAS) systems. Water Research, 46(16): 5085–5101

Martínez J L (2008). Antibiotics and antibiotic resistance genes in natural environments. Science, 321(5887): 365–367

Michael I, Rizzo L, Mcardell C S, Manaia C M, Merlin C, Schwartz T, Dagot C, Fatta-Kassinos D (2013). Urban wastewater treatment plants as hotspots for the release of antibiotics in the environment: a review. Water Research, 47(3): 957–995

Nguyen T T, Bui X T, Luu V P, Nguyen P D, Guo W, Ngo H H (2017). Removal of antibiotics in sponge membrane bioreactors treating hospital wastewater: comparison between hollow fiber and flat sheet membrane systems. Bioresource Technology, 240: 42–49

Nguyen V, Karunakaran E, Collins G, Biggs C A (2016). Physicochemical analysis of initial adhesion and biofilm formation of *Methanosarcina barkeri* on polymer support material. Colloids and Surfaces. B, Biointerfaces, 143: 518–525

Porras J, Bedoya C, Silva-Agredo J, Santamaria A, Fernandez J J, Torres-Palma R A (2016). Role of humic substances in the degradation pathways and residual antibacterial activity during the photodecomposition of the antibiotic *Ciprofloxacin* in water. Water Research, 94: 1–9

Su Z, Chen L, Wen D (2024). Impact of wastewater treatment plant effluent discharge on the antibiotic resistome in downstream aquatic environments: a mini review. Frontiers of Environmental Science & Engineering, 18(3): 36

Tang M, Zhou S, Huang J, Sun L, Lu H (2022). Stress responses of sulfate-reducing bacteria sludge upon exposure to polyethylene microplastics. Water Research, 220: 118646

Tran N H, Reinhard M, Gin K Y (2018). Occurrence and fate of emerging contaminants in municipal wastewater treatment plants from different geographical regions: a review. Water Research, 133: 182–207

Xu J, Sheng G P, Ma Y, Wang L F, Yu H Q (2013). Roles of extracellular polymeric substances (EPS) in the migration and removal of sulfamethazine in activated sludge system. Water Research, 47(14): 5298–5306

Yi K, Wang D, Yang Q, Li X, Chen H, Sun J, An H, Wang L, Deng Y, Liu J, Zeng G (2017). Effect of ciprofloxacin on biological nitrogen and phosphorus removal from wastewater. Science of the Total Environment, 605–606: 368–375

Zhang L, Song Z, Dong T, Fan X, Peng Y, Yang J (2023). Mitigating mechanism of nZVI-C on the inhibition of anammox consortia under long-term tetracycline hydrochloride stress: Extracellular polymeric substance properties and microbial community evolution. Journal of Hazardous Materials, 452: 131035

Zhang Q Q, Ying G G, Pan C G, Liu Y S, Zhao J L (2015). Comprehensive evaluation of antibiotics emission and fate in the river basins of China: source analysis, multimedia modeling, and linkage to bacterial resistance. Environmental Science & Technology, 49(11): 6772–6782

Zhao T, Liu X, Huai L, Feng R, Yan T, Xu W, Zhao Y (2024). Fabrication of the TiO_2/Ti_3C_2 loaded ceramic membrane targeting for photocatalytic degradation of PPCPs: ciprofloxacin, tetracycline, and ibuprofen. Frontiers of Environmental Science & Engineering, 18(10): 123

Zhou H, Li X, Chu Z, Zhang J (2016). Effect of temperature downshifts on a bench-scale hybrid A/O system: process performance and microbial community dynamics. Chemosphere, 153: 500–507